Future Energy Open Access Journal

ISSN 2832-0328

Journal homepage: https://fupubco.com/fuen



https://doi.org/10.55670/fpll.fuen.5.1.1

Article

Effect of piston bowl geometry on combustion, performance, and emission characteristics of a dual-fuel engine

Abdullah Al Rifat, Md. Mizanur Rahman, Md. Arafat Rahman*

Department of Mechanical Engineering, Chittagong University of Engineering and Technology, Chittagong-4349, Bangladesh

ARTICLE INFO

Article history:
Received 05 August 2025
Received in revised form
14 September 2025
Accepted 30 September 2025

Keywords:

Piston bowl, Dual-fuel, Engine, Energy share, Combustion and emission

*Corresponding author Email address: arafat@cuet.ac.bd

DOI: 10.55670/fpll.fuen.5.1.1

ABSTRACT

The piston bowl shape plays a crucial role in turbulence, swirl, and subsequent fuel-air mixing, which in turn affect combustion, emissions, and performance attributes. A cylinder stepped and modified re-entrant combustion chamber was investigated through Ansys Forte 2023 R1 CFD software to analyze combustion, emission, and performance characteristics in a diesel-methane dual-fuel engine. Numerical investigation is performed under 0.44 MPa load, 50% methane energy contribution, 7° start of injection bTDC, and with a 120° spray angle. Methane is injected into the inlet manifold to be premixed with air. The maximum thermal efficiency was found to be 34.11%, and a specific fuel consumption of 270.44 g/kW-h was indicated by the modified re-entrant bowl shape. The combustion duration for a modified re-entrant is 6.73% and 14.38% higher than that of a cylinder and stepped bowl. Higher combustion efficiency, combustion duration, and total apparent heat release demonstrate sustained combustion in the modified re-entrant bowl. Strong early premixed combustion in a cylinder-shaped bowl gives the highest percentage of NOx. The stepped bowl has fuel-rich zones near the center after 19° CA, with lower temperatures near the center, giving higher amounts of UHC and VOC emissions. The amount of O and OH radical formation in the modified re-entrant bowl was lower, and delayed oxidation resulted in a higher amount of CO emission. The modified reentrant bowl offered the best combustion, performance, and emission attributes among the bowl shapes.

1. Introduction

Internal combustion engines (ICE) persist as a significant part of the energy cycle. The global impact of vehicle emissions on the environment is increasing. ICEs must meet high-performance and minimal-emission regulations, which complicates engine design [1]. Engine manufacturers have expanded their research on reducing exhaust emissions in response to growing awareness of air pollution and increasingly restrictive emission regulations. In addition, several studies are conducted on the parameters that influence the performance of engines and combustion [2]. The efficiency, combustion characteristics, and emissions of a compression ignition engine are influenced by various factors, including fuel standards, operating conditions, and engine structural design [3]. A more rapid and efficient blend of air and fuel is the most significant requirement for lowering exhaust emissions, boosting engine performance, and enhancing combustion characteristics [4]. The piston bowl, or upper section of the piston, creates the combustion chamber

alongside the cylinder bowl. The design of the piston bowl alters the turbulent nature of the flow and the consistency of the air-fuel mixture [1]. Improving the geometry of the combustion space, adjusting injection parameters, and optimizing air movement characteristics can enhance the mixing ability of diesel fuel with air. For optimal geometry, the ratio of air to fuel should be adjusted, and for better evaporation, there ought to be greater circulation of air in the cylinder in the form of swirl, squish, and turbulence [2]. The effect of piston bowl shape on engine flow, turbulence, mixing, and burning has been widely studied in the literature [5-11]. Advances in fuel-air mixing across the cylinder have an opportunity to significantly improve combustion and thereby increase engine performance [12]. The gas flow inside the cylinder is primarily influenced by swirl alongside turbulent kinetic energy, which in turn affects flame propagation [13]. Over the last decade, researchers have shown a strong interest in diesel engine combustion chamber design, which offers various approaches for enhancing airflow within the engine's cylinders. Optimal bowl shape increases air/fuel mixture creation while reducing rich regions [14]. Both nitrogen oxide (NO_x) emissions and local temperature rise can be reduced by eliminating rich mixing regions [15]. The impact of combustion chamber shape on the performance of the engine, flow field, and air-fuel interaction is extremely complex. The ICEs intricate structure has hampered experimental studies into the shape of the piston bowl. The investigation will be costly and time-consuming. As a result, numerical modeling has become a helpful tool for evaluating and improving engine control systems due to its greater versatility and lower cost when compared to experimental approaches [16].

Kakaee et al. [17] studied numerically three piston bowl shapes, namely stock, bathtub, and cylindrical, in a diesel engine at medium load. Reported that the bathtub shape turned out to have the best performance and emission values. The bowl profile did not significantly affect the combustion of the reactivity-controlled compression ignition (RCCI) engine at low engine speeds, but it had a substantial impact at higher engine speeds. The bowl profile had a considerable effect on NOx, but a negligible effect on unburned hydrocarbons (UHC) and carbon monoxide (CO). Singh et al. [18] studied various combustion chamber shapes, finding that the required tumble, swirl, squish, and turbulence attributes in the chamber can be enhanced, resulting in lower emissions and improved performance. The re-entrant piston bowl is best for generating turbulent kinetic energy and swirl during the compression stroke. Hariharan et al. [19] studied with reentrant bowl and shallow bowl geometry. Under identical conditions, there was a slight variation in the combustion aspect between these two geometries; however, the shallow bowl design performed somewhat better in terms of thermal efficiency.

Saito et al. [20] evaluated traditional and re-entrant bowls in a diesel engine to evaluate performance, emissions, and combustion characteristics. Consequently, the ignition delay is minimized because the re-entrant configuration is hotter than the opposite wall where the fuel strikes. Furthermore, as the number of air motions in the cylinder increased, turbulence also increased, and combustion attributes improved. Gülcan and Ciniviz [10] studied the effects of toroidal and toroidal re-entrant chamber geometry on a methane diesel engine. The testing results revealed that the toroidal re-entrant combustion chamber (TRCC) design eliminates the long ignition delay caused by methane addition and provides more stable combustion under all torque settings. In summary, the TRCC geometry has been demonstrated to be a practical approach for achieving improved combustion and reduced emission levels in dual fuel mode under torque conditions ranging from 3 to 9 Nm. Yaliwal et al. [21] found that the re-entrant design combustion chamber performed best at an injection pressure of 23 MPa and a nozzle opening of 0.25 mm, with 4 holes. Dempsey et al. [22] demonstrated that at a low load, the shallow cylinder has much higher combustion efficiency than the re-entrant bowl piston due to lower heat transfer losses and greater combustion efficiency. Using the typical reentrant piston bowl design, these fuel combinations achieve minimal NO_x and particulate matter (PM) emissions while reaching a maximum gross required efficiency of 48%. Over the whole load and speed range, the redesigned piston produced minimal NO_x and PM emissions, with a peak gross stated efficiency of around 51%. Bapu et al. investigated the Modified Hemispherical Combustion Chamber (MHCC) and traditional Hemispherical Combustion Chamber (HCC)

designs in a diesel engine using ANSYS Fluent software. According to the results, mixing was improved when flow motions at different places of the piston were studied instead of the HCC [23]. Pham et al. [24] studied the impact of piston bowl shape on combustion and emissions in a heavy-duty marine diesel engine. Three different piston bowl configurations were numerically investigated. The study found that ω-type and re-entrant piston chambers increased cylinder power and decreased specific fuel consumption compared to U-type chambers. ω-type and re-entrant piston heads have lower peak temperatures than U-type piston crowns, resulting in decreased NO_x emissions. Piston bowl design was also discovered to have no influence on soot and carbon dioxide (CO₂). The application of re-entrant piston chambers is strongly suggested for improving engine efficiency and fuel economy while lowering nitrogen monoxide (NO) emissions.

Mobasheri and Peng [25] employed computational fluid dynamics (CFD) modeling to investigate the impact of a reentrant chamber on mixture preparation, combustion, and engine performance. When determining the influence of the combustion chamber, thirteen alternative designs were analyzed and categorized into four key aspects: bowl depth, breadth, bottom surface, and lip area. The findings indicated that the shape of the combustion chamber has a substantial impact on the combustion process. It was demonstrated that by modifying the shape of the bowl, the level of emission pollutants could be lowered while other engine performance metrics remained constant. The purpose of this research is to assess the performance, combustion, and emission characteristics of a dual-fuel diesel engine with different piston bowl shapes via ANSYS Forte 2023 R1 CFD numerical software. While piston bowl design has a substantial impact on air-fuel mixing, ignition delay, and combustion parameters in diesel engines, it draws little attention in studies of methane-diesel dual-fuel combustion. This study conducts a complete CFD-based analysis of various bowl shapes to determine their effects on in-cylinder pressure, thermal efficiency, and emissions. The findings demonstrate the piston bowl effect as a viable strategy for enhancing performance and lowering emissions in dual-fueled engines.

2. Computational methodology

2.1 Governing equation

The gas-phase working fluids are modeled using a mixture of several gas species in CFD. The continuity equation for a whole gas-phase fluid can be obtained by combining the equations for all species. Their composition changes while the engine is running due to molecular diffusion, flow convection, turbulence transport, contact with fuel sprays, and combustion. Governing equations are essentially dictated by the perfect gas law during the gas phase, Newtonian fluid dynamics, Fick's law governing mass diffusion, and Fourier's law governing thermal diffusion. The species conservation equation [26] is stated in Eq (1). Here, n=1, 2, ... N, subscript n is the species index, N is the total species number, $\tilde{\rho}$ is the density, \bar{v} is the velocity, $y_n = \frac{\rho_n}{\rho}$ is the mass fraction of species n; and $\tilde{\rho}_n^c$ and $\tilde{\rho}_n^s$ are chemical reactions and spray evaporation terms, respectively. The term, ϕ is the effect of the ensemble's mean convection factor [27] stated in Eq (2).

$$\frac{\delta \tilde{\rho}_n}{\delta t} + \nabla \cdot (\tilde{\rho}_n \bar{v}) = \nabla \cdot [\tilde{\rho} D \nabla \tilde{y}_n] + \nabla \cdot \phi + \tilde{\rho}_n^c + \tilde{\rho}_n^s$$
 (1)

$$\phi = \tilde{\rho}_n \bar{v} - \overline{\rho_n v} \tag{2}$$

The continuity equation of the gas phase fluid is stated in Eq (3) [27,28].

$$\frac{\delta \tilde{\rho}}{\delta t} + \nabla \cdot (\tilde{\rho} \, \bar{v}) = \tilde{\rho}^{\,s} \tag{3}$$

Equation (4) is the momentum equation used in Ansys Forte, which accounts for convection, pilot fuel spray, viscous stress, pressure force, gravity force, and turbulence transport effect [26]. Where, \bar{p} , \bar{F}^s , \tilde{I} and \bar{g} are the pressure, momentum gain rate for spray per unit volume, stress due to the effects of ensemble-averaging the nonlinear convection, and body force, respectively. The viscous shear stress, $\tilde{\sigma}$, is stated in Eq. (5) where, \tilde{I} and v accounts for the identity tensor and kinematic viscosity, respectively.

$$\frac{\delta \tilde{\rho} \bar{v}}{\delta t} + \nabla \cdot (\tilde{\rho} \bar{v} \bar{v}) = -\nabla \bar{p} + \nabla \cdot \tilde{\sigma} - \nabla \cdot \tilde{\Gamma} + \bar{F}^s + \tilde{\rho} \bar{g}$$
(4)

$$\tilde{\sigma} = \tilde{\rho}v \left[\nabla \bar{v} + (\nabla \bar{v})^T - \frac{2}{3} (\nabla \bar{v})\tilde{I} \right]$$
 (5)

From 1st law of thermodynamics, a change in internal energy needs to be equalized by pressure work and heat transfer. Eq (6) is the internal energy transport mathematical equation [27,28]. Where, $\tilde{u},\hat{\varepsilon},\bar{Q}_r,\bar{q}$ and $\tilde{\mathbf{H}}$ are the specific internal energy, dissipation rate, radiation heat loss, heat flux vector and effect of convection parameter filtering, respectively. The \bar{Q}^c and \bar{Q}^S are the source effects due to chemical heat release parameters and spray interactions, respectively.

$$\frac{\delta \tilde{\rho} \tilde{u}}{\delta t} + \nabla \cdot (\tilde{\rho} \bar{v} \tilde{u}) = -\bar{p} \nabla \cdot \bar{v} - \nabla \cdot \bar{q} - \nabla \cdot \tilde{H} + \tilde{\rho} \hat{\epsilon} + \tilde{Q}^c + \tilde{Q}^S - \tilde{Q}_r$$
(6)

The flow turbulence model is for solving the Reynolds-averaged Navier-Stokes (RANS) equations. The focus of RANS is to simulate the ensemble-mean flow. The ensemble is an average that enables the understanding of incidents depending on the repeatability of multi-component flow streams. The Reynolds stress tensor, $\tilde{\Gamma}$, and the turbulent kinematic viscosity, v_T , are shown in Eqs (7) and (8), respectively [27], where, C_{μ} is the model constant that varies with various turbulence models. The turbulent kinetic energy, $\widetilde{k_e}$, is represented in Eq (9) [29].

$$\tilde{I} = -\tilde{\rho} v_T \left[\nabla \bar{v} + (\nabla \bar{v})^T - \frac{2}{3} (\nabla \bar{v}) \tilde{I} \right] + \frac{2}{3} \tilde{\rho} \widetilde{k_e} \tilde{I}$$
(7)

$$v_T = C_\mu \frac{\widetilde{k_e}^2}{\widehat{c}} \tag{8}$$

$$\widetilde{k_e} = \frac{1}{2\tilde{\rho}} trace \left(\tilde{\Gamma} \right) = \frac{1}{2} \overline{v} \cdot \overline{v}$$
 (9)

The turbulence flux parameter in the species transport numerical model [29] is represented in Eq. (10). Equations (11) and (12) refer to the turbulence flow factor, \widetilde{H} , [27], and the Reynolds stress, $\widetilde{\tau}$, respectively [28]. Where D_T and \overline{k}_{tc} are the turbulence diffusivity and turbulence thermal conductivity, respectively.

$$\phi = \tilde{\rho} D_T \nabla \bar{k}_{tc} \tag{10}$$

$$\widetilde{H} = -k\nabla \overline{T} - \widetilde{\rho} D_T \sum_n \widetilde{h}_n \nabla \overline{y}_n \tag{11}$$

$$\tilde{\tau}_r = \tilde{\rho}(\overline{v}\overline{v} - \bar{v}\overline{v}) \tag{12}$$

2.2 Bowl geometry and mesh

Three different piston bowl geometries, namely cylinder, stepped, and modified re-entrant, shown in Figure 1(a)-(c), respectively, are analyzed at 110° spray angle. To account for the symmetry of the combustion chamber, the bowl of eight injectors is divided into one-eighth sections. For injectors that

are uniformly spaced, factors like injection pressure, temperature, air-fuel mixing, and combustion events are considered to be similar across each hole in the injector and the corresponding spray [27]. In this study, the sector angle is set to 45°, having periodic boundary conditions applied at the periodic faces.

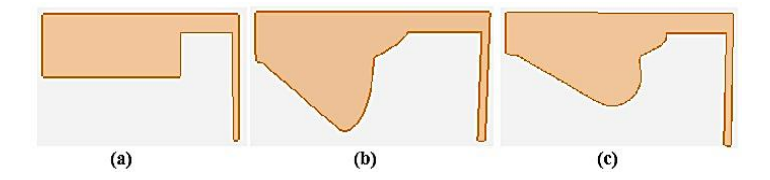


Figure 1. Piston bowl shape, (a) cylinder, (b) stepped, and (c) modified re-entrant

The peak cylinder pressure (PCP) values for the cylindershaped bowl model range from 7.78 MPa to 8.31 MPa, as illustrated in Figure 2(a). Mesh count 20600 has a PCP of 8.31 MPa and is used as the final mesh for modeling a cylindrical bowl. The PCP in a stepped bowl occurs at 15660 and 18375 mesh counts; these two PCP are close enough, and the highest is shown in Figure 2(b). The final mesh number for the stepped bowl is 18375. For the modified re-entrant bowl, mesh number 18120 is used for the final mesh. Hydrocarbon (HC) and CO pollutants firstly increased and then decreased over different methane energy share (MES), and a maximum reduction of NO_x by 35% at a 50% MES level [30]. CO decreased when the MES was increased from 0 to 50%. CO emissions increase significantly as the MES reaches 75%. Methane absorbs a considerable portion of the oxygen inside the intake manifold, minimizing CO oxidation. At 75% MES, the diesel amount is extremely low to ensure complete combustion of methane, and it cannot burn on its own because of its greater auto-ignition temperature. Incomplete combustion causes higher CO emissions [31]. This study uses 50% MES to examine combustion, performance, and emissions. The engine operating conditions for the bowl shapes are given in Table 1.

Table 1. Engine parameters

Type of engine	Single cylinder, 4- stroke
Piston diameter	139.7 mm
Piston stroke	152.4 mm
Squish	5.6 mm
Connecting rod dimension	304.8 mm
Crevice width	1.67 mm
Crevice height	37.2621 mm
Geometric compression ratio	11.1957
Total nozzle count	8
Nozzle orifice diameter	0.1961 mm
Speed	1200 rpm
Start of diesel injection	−7° aTDC
Spray angle	110°
Inflow droplet temperature	384 K
Discharge co-efficient	0.7

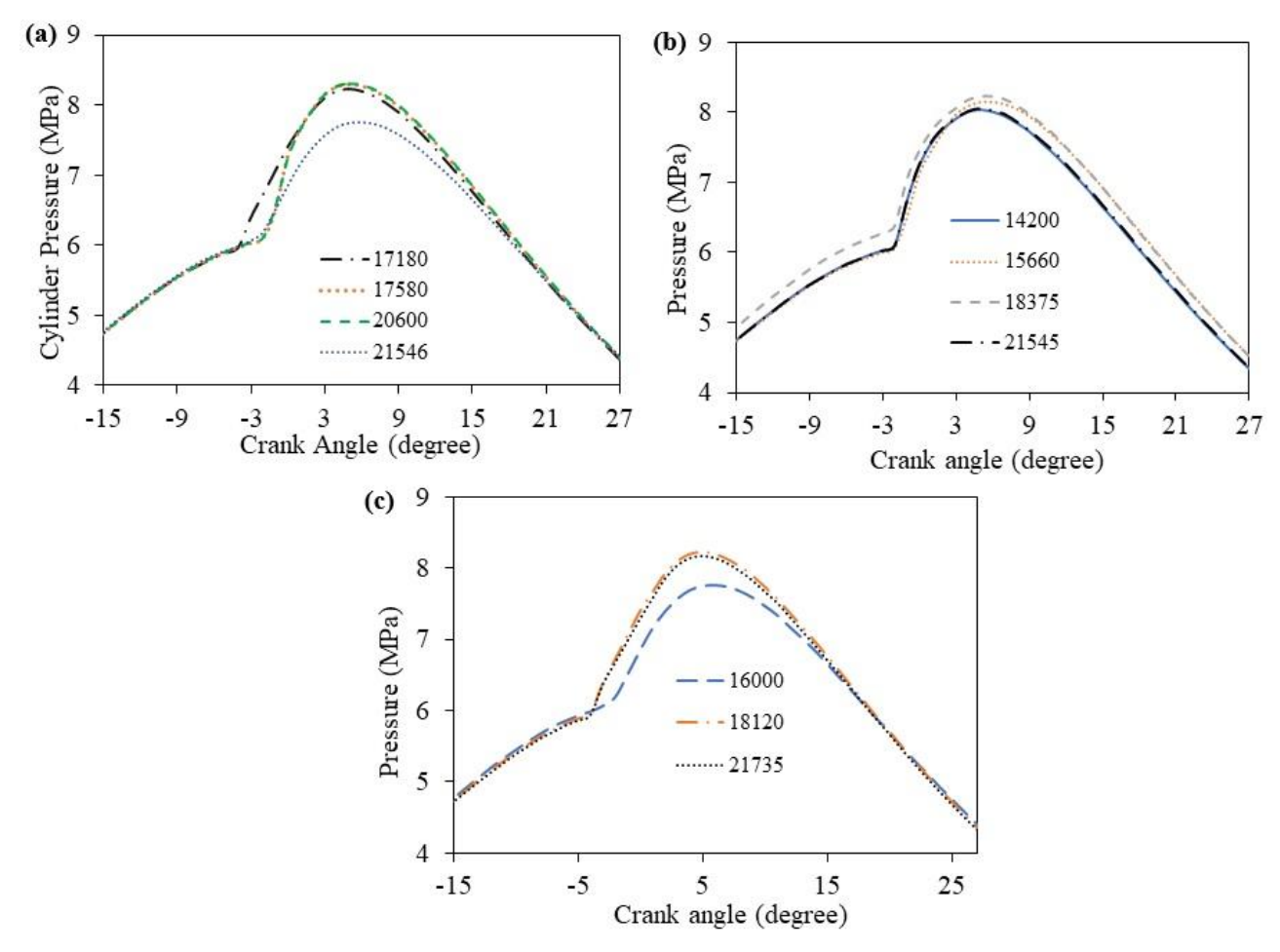


Figure 2. Optimum mesh: (a) Cylinder, (b) Stepped, and (c) Modified re-entrant

Table 2 demonstrates the initial and boundary conditions utilized in this simulation. These values are useful in scenarios involving three different piston bowl shapes. The piston, head, and liner all have a wall model, which allows for more accurate capture of the influence of the wall boundary layer.

2.3 Chemistry and sub-models

To set out the chemical reaction process for dual fuel combustion, a Chemkin file was developed by combining the diesel and methane Chemkin mechanism data with the CHEMKIN 2023 R1. The n-heptane [32] describes how diesel fuel burns in a conventional diesel engine. The GRI-Mech 3.0 [33] is a popular chemical kinetics instrument for modeling methane combustion. The total number of species and reactions was below the individual sums of the two processes. The explanation is that both processes contain the same species and reactions. This merged Chemkin file is added to the chemical set in the chemistry model. Table 2 lists some of the other CFD sub-models required for this study.

2.4 Model validation

The numerical findings of PCP for diesel combustion are then compared with in-cylinder pressure by Musculus's reported data [34], demonstrating appropriate consistency as shown in Figure 3. The PCP fluctuations of approximately 2.45% were discovered when compared to the current study.

 $\textbf{Table 2.} \ \textbf{Initial and boundary conditions}$

Parameters	Correspondent data
Intake valve closing	165° bTDC
Exhaust valve opening	125° aTDC
Intake pressure	2.33 bar
Intake mixture temperature	384 K
Primary swirl ratio	0.5
Primary swirl shape factor	3.11
Turbulent kinetic energy	10,000 cm ² /sec ²
Wall temperature of piston	400 K
Head temperature of piston	375 K
Liner temperature of piston	365 K

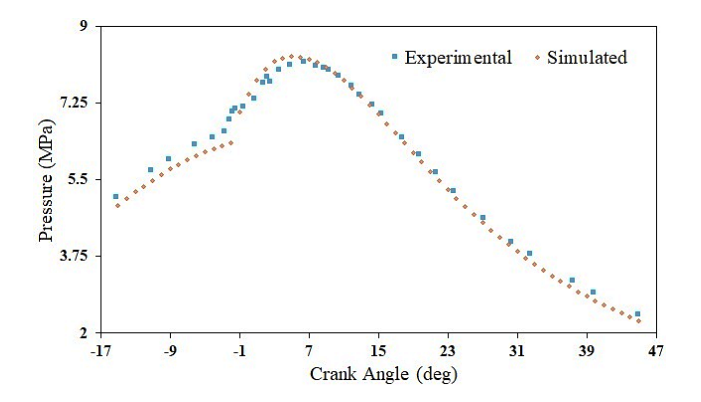
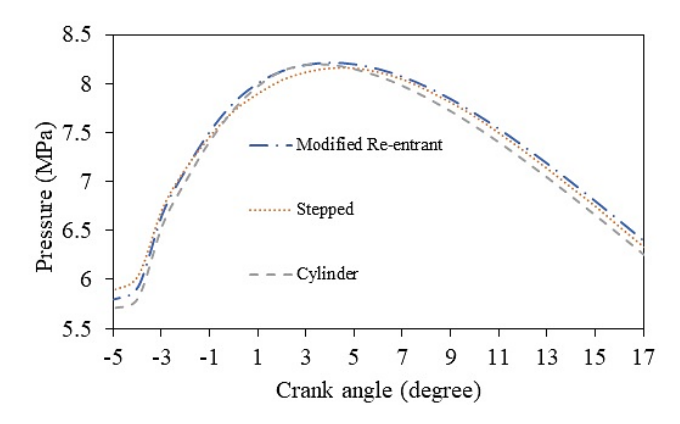


Figure 3. Validation for cylinder pressure with Musculus

3. Results and discussion

3.1 Bowl shape effect on combustion

The PCP of the modified re-entrant bowl is 0.28% and 0.7% higher than the cylinder and stepped bowl, respectively. The highest PCP of modified re-entrants suggests an early start of combustion. The area under the cylinder pressure (CP) and crank angle (CA) demonstrates the net release of heat during combustion. Figure 4 represents CP variation for three different bowl shapes. The modified re-entrant bowl promotes more complete burning compared with the cylinder and stepped bowl. The uniform pressure variation of the modified re-entrant suggests turbulence increased in the combustion chamber, which enhances mixing of the premixed charge and diesel. The peak cylinder temperature (PCT) of the modified re-entrant shape is 1.24% and 0.46% higher than that of the cylinder and stepped bowl, respectively. Figure 5 represents cylinder temperature variation over crank angle. The modified re-entrant bowl leads to more efficient heat transfer inside the combustion chamber. Improved mixing and turbulence can lead to higher PCT. The peak apparent heat release rate (AHRR) is 0.075% and 9.53% higher in cylinder shape than in the modified re-entrant shape and steeped, respectively. The peak AHRR in the cylinder and the modified re-entrant shape are almost the same. AHRR for the three bowl shapes is shown in Figure 6 at various CA. From -5° CA to -1.75° CA, AHRR increases and then decreases at the same rate; and at this range, values are close enough for both the modified re-entrant and cylinder shapes. After -1.75° to 3° CA, the AHRR curve for the cylinder shape is above the modified re-entrant. After 3° CA, the AHRR curve of the modified re-entrant curve surpasses the cylinder bowl.



 $\label{eq:Figure 4.} \textbf{In-cylinder pressure variation for three different piston bowl shapes}$

This phenomenon exhibits weaker swirl, less turbulence, and early burning of the premixed phase, resulting in weaker diffusion-controlled combustion. The modified re-entrant bowl enhances air-fuel mixing, allowing more of the methaneair mixture to participate in sustained combustion after the premixed phase. The total apparent heat release (AHR) for the modified re-entrant is 8.07% and 2.74% higher than the cylinder and stepped bowl, respectively, as shown in Figure 7(d). The longest duration for combustion is for the modified re-entrant shown in Figure 7(b) and is for a maximum heat release of 2046.18 I. During the premixed phase, the combustion fuel burns rapidly. Main diffusion phase combustion, which follows the premixed phase, is related to combustion duration with heat release rate (HRR) [35]. Combustion efficiency (CE) of the modified re-entrant is 2.12% and 7.41% higher than that of the cylinder and stepped chamber, respectively, as shown in Figure 7(a). The 10% to 90% heat release duration for the modified re-entrant is 6.73% and 14.38% higher than that for the cylinder and stepped bowl, respectively, as shown in Figure 7(b). Lower combustion duration (CD) signifies a short diffusion stage of combustion and improved premixed phase combustion [36]. A longer duration of heat release and the highest CE indicate sufficient time to oxidize fuel, more sustained combustion, and an increase in total heat release. For the stepped bowl, the peak AHRR, CE, and CD are lower than for the cylinder shape, but the total AHR is 5.19% higher.

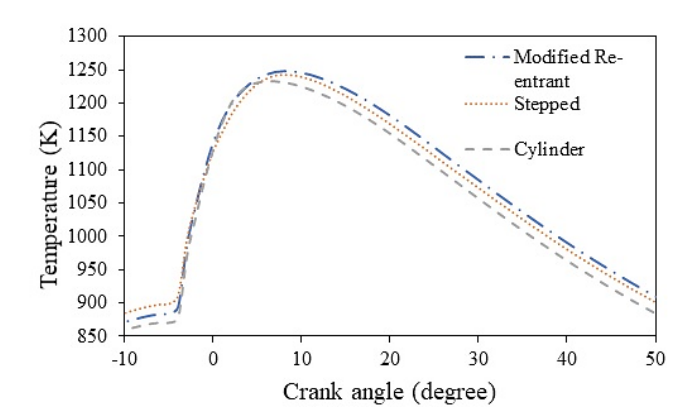


Figure 5. Cylinder Temperature variation for three different piston bowl shapes

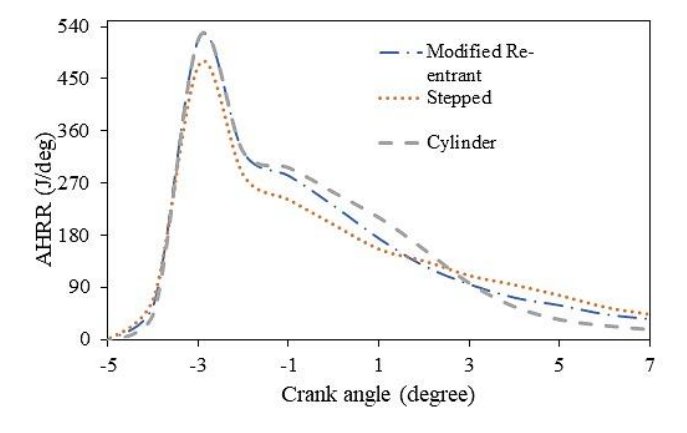


Figure 6. AHRR variation for three different piston bowl shapes

CE demonstrates how much chemical energy is released from fuel into useful work. CE for stepped bowl signifies mixing is poor and a larger amount of fuel is oxidizing incompletely. Figure 9 shows the highest percentage of UHC and VOC emissions from the stepped bowl. A strong late diffusion burn can give a large area under the AHRR curve without a significant amount of complete oxidation. Peak pressure rise rates (PPRR) are almost the same for both the cylinder and the modified re-entrant bowl, as shown in Figure 7(c). The modified re-entrant bowl has high PPRR with high CE. Besides, the cylinder has similar PPRR, but less overall oxidation, demonstrating it is less favorable than the modified re-entrant bowl.

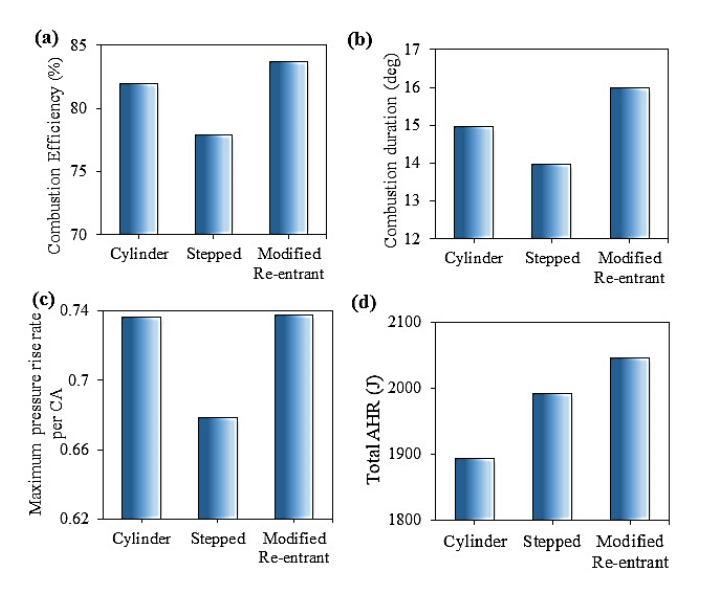


Figure 7. Comparison of, (a) combustion efficiency, (b) combustion duration, (c) maximum pressure rise rate, and (d) total AHR for three different bowl shapes

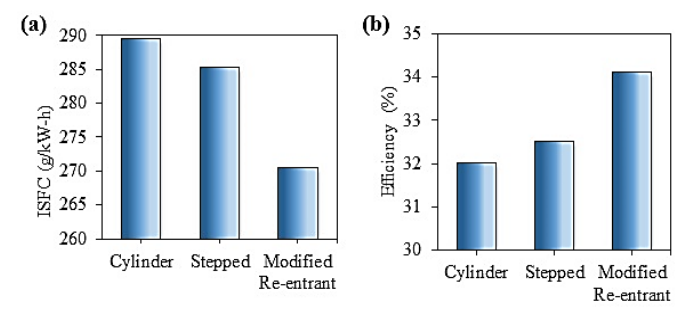
3.2 Bowl shape effect on performance

The amount of fuel consumed per kWh is indicated by specific fuel consumption (ISFC). The ISFC is 1.5% and 7.05% higher in the cylinder bowl than in the stepped and modified re-entrant shapes, respectively, as shown in Figure 8 (a). Thermal efficiency is the fraction of fuel energy that is converted into work. The thermal efficiency for the modified re-entrant is 4.86% and 6.5% higher than the stepped and cylinder bowl, respectively, as shown in Figure 8 (b). Enhanced swirl and turbulence are generated by the reentrant lip, which improves mixing and sustained oxidation during the diffusion phase in the modified re-entrant bowl. A modified re-entrant bowl yields lower ISFC and higher thermal efficiency, enabling a significant fraction of chemical energy to be converted into useful work. Despite the intermediate CE and CD of the cylinder bowl, it has a higher ISFC and lower thermal efficiency. The rapid burning of premixed fuel increases NOX, as shown in Figure 9 for the cylinder bowl shape, and weaker diffusion burn decreases total AHR, as shown in Figure 7(d).

3.3 Bowl shape effect on emission

 NO_x emissions of the cylinder bowl are 15.91% and 15.16% higher than those of the stepped and modified reentrant bowls, respectively, as shown in Figure 9. The PCT of the modified re-entrant shape is 1.24% and 0.46% higher, and the PCP is 0.28% and 0.7% higher than the cylinder and stepped bowl, but NO_X emission is higher in the cylinder bowl.

The PCT and PCP differences are not enough to define NO_x formation dependency due to temperature. In the cylinder bowl, PCP and PCT occurred at 3° CA and 4° CA, respectively. as in Figure 5. But, in the modified re-entrant bowl, PCP and PCT occurred at 4° CA and 7° CA, respectively, and in the stepped bowl, they occurred at 4° CA and 6° CA, respectively. The cylinder-shaped bowl's PCP and PCT occurred earlier, close to top dead center (TDC), and PPRR was also high. Early PCP and PCT conditions strongly favor Zeldovich thermal NO_x formation. Early PCP and PCT with PPRR indicate a very fast premixed burn near TDC. Although the modified re-entrant has a longer CD than the cylinder bowl, the stronger, earlier, and instantaneous combustion in the cylinder bowl provides a larger integrated NO_x. The superior mixing inside the modified re-entrant shape lowers local fuel-rich hot spots; this lowers local NO_x formation.



 $\textbf{Figure 8.} \ Comparison \ of (a) \ ISFC, and (b) \ thermal \ efficiency, for \ three \ different bowls$

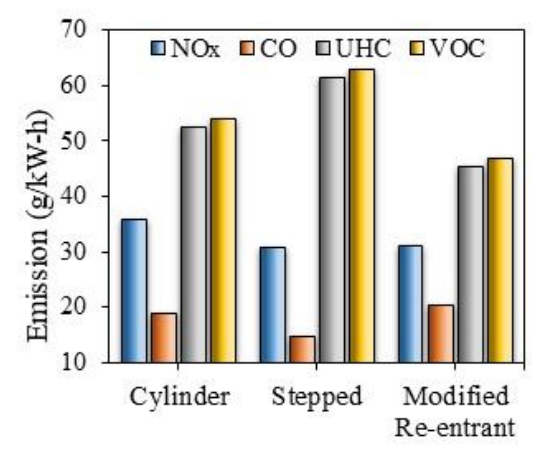


Figure 9. Comparison of emissions for three different piston bowl shapes at $0.44~\mathrm{MPa}$ load

The CO emission of the modified re-entrant is 6.32% and 37.41% higher than that of the cylinder and stepped bowl, respectively, as shown in Figure 9. The presence of highly active 0 and OH free radicals increases the oxidation of CO into CO₂ [37,38]. Figure 10 shows the active 0 and OH radicals for three different bowls. From -165° CA to 125° CA simulation, the stepped bowl has a higher amount of 0 and OH radical formation than the cylinder bowl, and then the modified re-entrant bowl shape. As free radical formation is lower in the modified re-entrant, CO emission is higher, as shown in Figure 9. CO emission is lower in stepped bowls due to higher 0 and OH radicals. In a steeped bowl, though radical formation is delayed, the cumulative radical formation is large and effectively converts CO into CO₂.

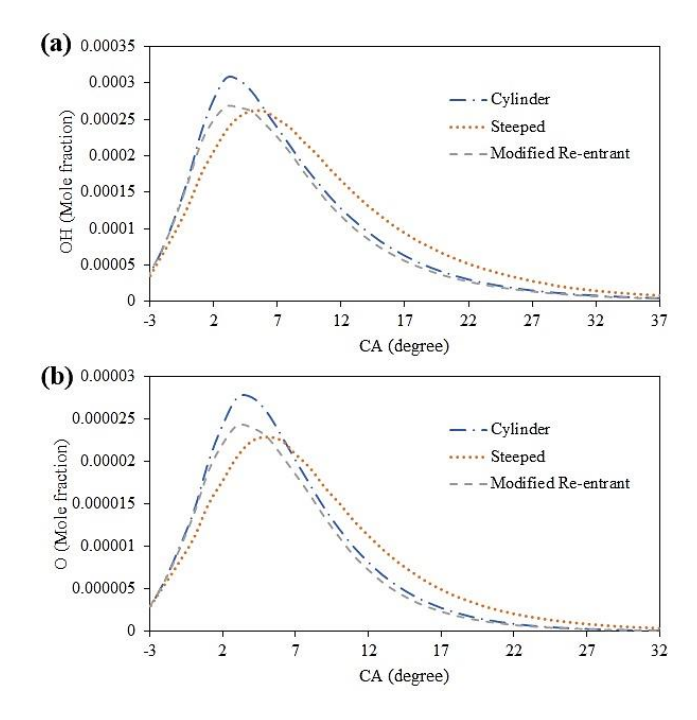


Figure 10. Reactive species, (a) OH radical, and (b) O radical

The UHC emission of the stepped bowl is 17% and 35.62% higher than that of the cylinder and modified reentrant bowl, respectively, as shown in Figure 9. A modified re-entrant bowl enhances very good mixing, and a longer CD and total AHR demonstrate a sustained diffusion phase and enable more oxidation, which lowers UHC. A short CD in a stepped bowl means weak diffusion-controlled combustion. The VOC emission of the stepped bowl is 16.48% and 34.4% higher than that of the cylinder and modified re-entrant bowl, respectively, as shown in Figure 9. VOC evaporates easily, and UHC is a specific type of VOC that results from the byproduct of incomplete combustion.

3.4 Qualitative analysis

At 3° CA, the stepped bowl has a higher small fuel vapor mass fraction (FVMF) shown in Figure 11, which demonstrates that locally rich pockets remained unmixed into oxidant streams. The cylinder and modified re-entrant have fewer pockets; comparing these two, the modified reentrant provides slightly better mixing. At 7° CA, there are local rich hot zones for the cylinder and stepped bowl, and the rich cold zones of the steeped are highest at the head. Overall, FVMF is the highest in the stepped bowl and then the cylinder bowl. From 11° to 19°, FVMF pockets almost remained unreacted by the cylinder and stepped bowl; that is a sign of much lower diffusion oxidation. FVMF still burns slowly from 11° CA to 19° CA, suggesting sustained diffusion oxidation. All bowls showed the FVMF reduction towards the centerline. FVMF concentrated near the cylinder axis much more for the stepped, then the cylinder, and then the modified re-entrant bowl. The modified re-entrant bowl better summarizes net mixing and steps down the lower net mixing. Piston bowls showed higher and wider temperature distribution along the spray direction, as shown in Figure 12, representing the premixed combustion region. The stepped bowl has a higher temperature zone near the bowl axis for 3° CA. At 11° CA, bowls have hot spots at the center, and stepped bowls show higher temperature distribution at the center.

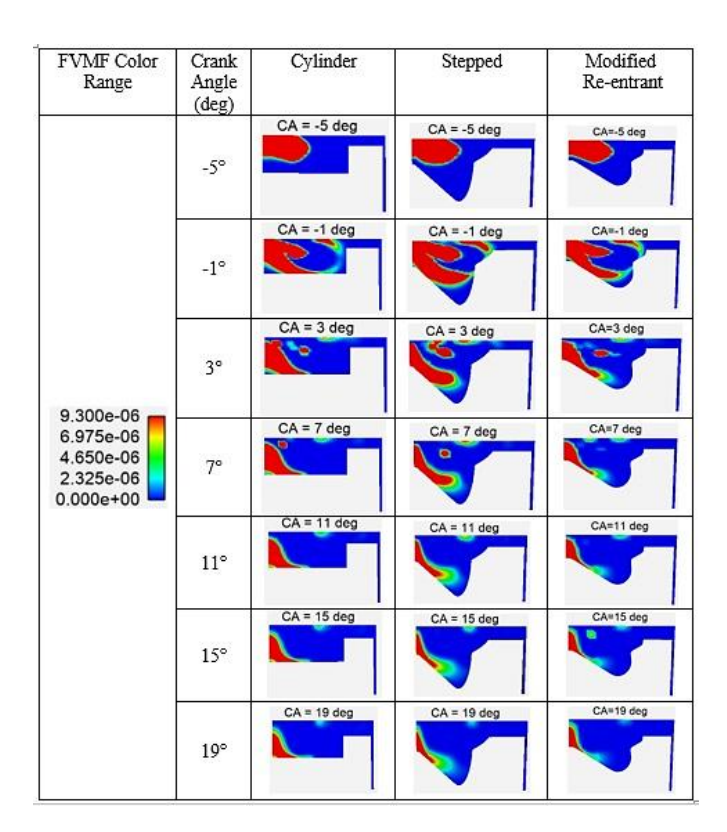


Figure 11. Fuel vapor mass fraction for different piston bowl shapes

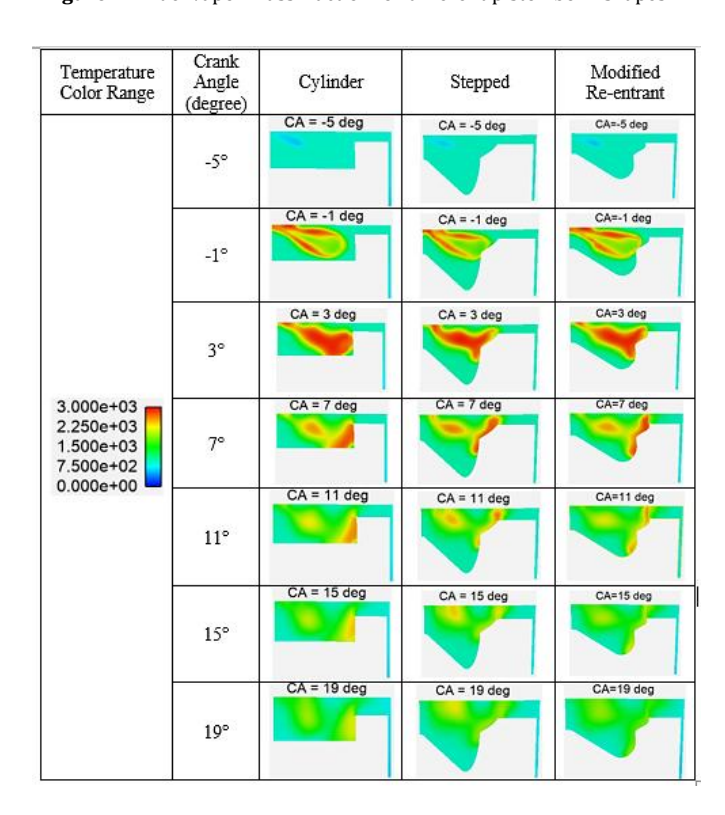


Figure 12. Temperature distribution for three different piston bowl shapes

The stepped bowl has a hot spot at the squish zone and has a higher temperature distribution along the step curvature, but a much lower temperature distribution at the bowl radius periphery. The modified re-entrant bowl showed the higher temperature distribution along the bowl radius periphery and in the squish zone. Cylinder bowls have a much higher temperature distribution along the lower bowl depth surface. At 19° CA, the modified re-entrant maintains a wide and uniform range of higher temperatures, reflecting sustained diffusion oxidation. Around 3° CA, early wide hotspots with high PPRR produce higher amounts of thermal NO_x. The contours demonstrate that the stepped bowl captures and maintains higher fuel vapor in the near middle, which remains unreacted because of the short diffusion phase and causes higher UHC and VOC levels. The cylinder generates intense, early hotspots that cause the greatest NO_x levels, while its weaker diffusion burns result in modest UHC. The modified re-entrant generates a more uniform vapor distribution and sustains late oxidation, decreasing UHC and VOC and boosting thermal efficiency.

4. Conclusion

This study investigates how a dual-fuel (DF) engine at 50% MES is affected by different bowl geometries on combustion, emission, and performance attributes. The piston bowls are investigated with 45° sections for eight injectors with periodic boundary conditions at the periodic faces to reduce computational time. Ansys Forte 2023 R1 software was used for the analysis of the cylinder, stepped, and modified re-entrant bowl. There are some observations that have been found in this investigation as follows:

- Modified re-entrant's longer combustion duration with higher combustion efficiency indicates enough time to oxidize fuel, more sustained combustion, and an increase in total heat release. For the stepped bowl, the peak AHRR, combustion efficiency, and combustion duration are lower than those of the cylinder shape, but the total AHR is 5.19% higher. The cylinder bowl has a similar PPRR but less overall oxidation, demonstrating it is less favorable than the modified re-entrant bowl.
- The modified re-entrant bowl has the highest thermal efficiency with lower ISFC. The enhanced swirl and turbulence in the modified re-entrant chamber improve mixing and sustained oxidation during the diffusion phase.
- ullet In the cylindrical bowl, NO_x emissions peaked. NOX emissions in stepped and modified re-entrant bowls are close enough. The UHC and VOC emissions peaked in the stepped bowl with a larger fraction; the modified reentrant bowl was the lowest by 35.62% and 34.4%, respectively. The modified re-entrant bowl has the lowest amount of free radical formation results and the highest amount of CO fraction.
- A larger amount of FVMF remained unreacted in the middle
 of the stepped chamber, and a low temperature
 distribution at 19° CA results in a higher percentage of UHC
 and VOC emissions. The temperature distribution from
 7°CA to 19°CA, modified re-entrant bowl, showed a stable
 and uniform temperature distribution throughout the
 combustion chamber, demonstrating diffusion burn is
 superior to the cylinder-shaped bowl.

It is noted that the best performance was shown by the modified re-entrant bowl. Its lower ISFC ensures the best fuel economy with higher combustion efficiency and thermal efficiency. Sustained diffusion burning confirms complete fuel oxidation; that's why there are lower UHC and VOC. The

only drawback is the higher CO emission for delayed oxidation.

Acknowledgements

This work is financially supported by Chittagong University of Engineering & Technology (CUET), Bangladesh through research grant no. CUET/CHSR-47-47.4.11. The corresponding author is responsible for ensuring that the descriptions are accurate and agreed by all authors.

Ethical issue

The authors are aware of and comply with best practices in publication ethics, specifically concerning authorship (avoidance of guest authorship), dual submission, manipulation of figures, competing interests, and compliance with policies on research ethics. The authors adhere to publication requirements that the submitted work is original and has not been published elsewhere in any language.

Data availability statement

The manuscript contains all the data. However, more data will be available upon request from the corresponding author.

Conflict of interest

The authors declare no potential conflict of interest.

References

- [1] H. Topkaya, M.Z. Işık, Y. Çelebi, H. Aydın, Numerical analysis of various combustion chamber bowl geometries on combustion, performance, and emissions parameters in a diesel engine, Int. J. Automot. Eng. Technol. 13 (2024) 63–72.
- [2] İ. Temizer, Ö. Cihan, Ö. Öncüoğlu, Numerical investigation of different combustion chamber on flow, combustion characteristics and exhaust emissions, Eur. Mech. Sci. 7 (2023) 7–15.
- [3] B. Challen, R. Baranescu, Diesel engine reference book, (No Title) (1999).
- [4] R.M. Montajir, H. Tsunemoto, H. Ishitani, T. Minami, Fuel spray behavior in a small DI diesel engine: effect of combustion chamber geometry, SAE Technical Paper, 2000. https://doi.org/10.4271/2000-01-0946
- [5] P. Prabhakaran, C.G. Saravanan, R. Vallinayagam, M. Vikneswaran, N. Muthukumaran, K. Ashok, Investigation of swirl induced piston on the engine characteristics of a biodiesel fueled diesel engine, Fuel 279 (2020) 118503.
- [6] I.H. Rizvi, R. Gupta, Numerical investigation of injection parameters and piston bowl geometries on emission and thermal performance of DI diesel engine, SN Appl. Sci. 3 (2021) 626.
- [7] X. Wang, H. Zhao, Effect of piston shape design on the scavenging performance and mixture preparation in a two-stroke boosted uniflow scavenged direct injection gasoline engine, Int. J. Engine Res. 22 (2021) 1484–1499.
- [8] O. Adeniyi, Numerical investigation on the effect of piston bowl geometry on combustion characteristics of a heavy-duty diesel engine, Mapta J. Mech. Ind. Eng. 3 (2019) 9–20.
- [9] G. Mittal, M. Subhash, M. Gwalwanshi, Effect of initial turbulence on combustion with ECFM-3Z model in a CI engine, Mater. Today Proc. 46 (2021) 11007– 11010.

- [10] H.E. Gulcan, M. Ciniviz, Experimental study on the effect of piston bowl geometry on the combustion performance and pollutant emissions of methanediesel common rail dual-fuel engine, Fuel 345 (2023) 128175.
- [11] J. V Pastor, A. García, C. Micó, F. Lewiski, A. Vassallo, F.C. Pesce, Effect of a novel piston geometry on the combustion process of a light-duty compression ignition engine: An optical analysis, Energy 221 (2021) 119764.
- [12] C.P.A. Gafoor, R. Gupta, Numerical investigation of piston bowl geometry and swirl ratio on emission from diesel engines, Energy Convers. Manag. 101 (2015) 541–551.
- [13] J.B. Heywood, Internal combustion engine fundamentals, McGraw-Hill Education, 2018.
- [14] R. Sener, M.U. Yangaz, M.Z. Gul, Effects of injection strategy and combustion chamber modification on a single-cylinder diesel engine, Fuel 266 (2020) 117122.
- [15] P. Dimitriou, W. Wang, Z. Peng, A piston geometry and nozzle spray angle investigation in a DI diesel engine by quantifying the air-fuel mixture, Int. J. Spray Combust. Dyn. 7 (2015) 1–24.
- [16] J. Zhao, R. Yang, Y. Yan, J. Ou, Z. Liu, J. Liu, Numerical study on the effect of injector nozzle hole number on diesel engine performance under plateau conditions, SAE Technical Paper, 2023.
- [17] A.-H. Kakaee, A. Nasiri-Toosi, B. Partovi, A. Paykani, Effects of piston bowl geometry on combustion and emissions characteristics of a natural gas/diesel RCCI engine, Appl. Therm. Eng. 102 (2016) 1462–1472.
- [18] P. Singh, S.K. Tiwari, R. Singh, N. Kumar, Modification in combustion chamber geometry of CI engines for suitability of biodiesel: A review, Renew. Sustain. Energy Rev. 79 (2017) 1016–1033.
- [19] D. Hariharan, M. Rahimi Boldaji, Z. Yan, B. Gainey, B. Lawler, Exploring the effects of piston bowl geometry and injector included angle on dual-fuel and singlefuel RCCI, J. Eng. Gas Turbines Power 143 (2021) 111013.
- [20] T. Saito, Y. Daisho, N. Uchida, N. Ikeya, Effects of combustion chamber geometry on diesel combustion, SAE Trans. (1986) 793–803.
- [21] V.S. Yaliwal, N.R. Banapurmath, N.M. Gireesh, R.S. Hosmath, T. Donateo, P.G. Tewari, Effect of nozzle and combustion chamber geometry on the performance of a diesel engine operated on dual fuel mode using renewable fuels, Renew. Energy 93 (2016) 483–501.
- [22] A.B. Dempsey, N.R. Walker, R. Reitz, Effect of piston bowl geometry on dual fuel reactivity controlled compression ignition (RCCI) in a light-duty engine operated with gasoline/diesel and methanol/diesel, SAE Int. J. Engines 6 (2013) 78–100.
- [23] B.R.R. Bapu, L. Saravanakumar, B.D. Prasad, Effects of combustion chamber geometry on combustion characteristics of a DI diesel engine fueled with calophyllum inophyllum methyl ester, J. Energy Inst. 90 (2017) 82–100.
- [24] V.C. Pham, J.K. Kim, W.-J. Lee, S.-J. Choe, V.V. Le, J.-H. Choi, Effects of Piston Bowl Geometry on Combustion

- and Emissions of a Four-Stroke Heavy-Duty Diesel Marine Engine, Appl. Sci. 12 (2022) 13012.
- [25] R. Mobasheri, Z. Peng, Analysis of the effect of reentrant combustion chamber geometry on combustion process and emission formation in a HSDI diesel engine, SAE Technical Paper, 2012.
- [26] W.P. Adamczyk, G. Kruczek, R. Bialecki, G. Przybyła, Application of different numerical models capable to simulate combustion of alternative fuels in internal combustion engine, Int. J. Numer. Methods Heat Fluid Flow 30 (2020) 2517–2534.
- [27] K.M. Rahman, Z. Ahmed, Combustion and emission characteristics of a diesel engine operating with varying equivalence ratio and compression ratio-A CFD simulation, J. Eng. Adv. 1 (2020) 101–110.
- [28] O. Zikanov, Essential computational fluid dynamics, John Wiley & Sons, 2019. ISBN-13: 978-1119474623
- [29] B. Sun, Revisiting the reynolds-averaged navierstokes equations, Open Phys. 19 (2022) 853–862.
- [30] O.H. Ghazal, Air pollution reduction and environment protection using methane fuel for turbocharged CI engines, J. Ecol. Eng. 19 (2018) 52–58.
- [31] G. Tripathi, P. Sharma, A. Dhar, Effect of methane augmentations on engine performance and emissions, Alexandria Eng. J. 59 (2020) 429–439.
- [32] H.J. Curran, P. Gaffuri, W.J. Pitz, C.K. Westbrook, A Comprehensive Modeling Study of n-Heptane Oxidation, Combust. Flame 114 (1998) 149–177. https://doi.org/https://doi.org/10.1016/S0010-2180(97)00282-4.
- [33] Z. Smith, G. P.; Golden, D. M.; Frenklach, M.; Moriarty, N. W.; Eiteneer, B.; Goldenberg, M.; Bowman, C. T.; Hanson, R. K.; Song, S.; Gardiner, W. C. Jr.; Lissianski, V. V.; Qin, GRI-Mech 3.0, Univ. California, Berkeley (1999). http://www.me.berkeley.edu/gri_mech/.
- [34] M.P.B. Musculus, On the correlation between NOx emissions and the diesel premixed burn, SAE Trans. (2004) 631–651.
- [35] S.M. Farhan, P. Wang, Post-injection strategies for performance improvement and emissions reduction in DI diesel engines—A review, Fuel Process. Technol. 228 (2022) 107145. https://doi.org/https://doi.org/10.1016/j.fuproc.20 21.107145.
- [36] C. Deheri, S.K. Acharya, D.N. Thatoi, A.P. Mohanty, A review on performance of biogas and hydrogen on diesel engine in dual fuel mode, Fuel 260 (2020) 116337. https://doi.org/https://doi.org/10.1016/j.fuel.2019. 116337.
- [37] Y. Sun, Y. Zhang, M. Huang, Q. Li, W. Wang, D. Zhao, S. Cheng, H. Deng, J. Du, Y. Song, Effect of hydrogen addition on the combustion and emission characteristics of methane under gas turbine relevant operating condition, Fuel 324 (2022) 124707.
- [38] G. Tripathi, A. Dhar, Performance, emissions, and combustion characteristics of methane-diesel dual-fuel engines: A review, Front. Therm. Eng. 2 (2022) 870077.



This article is an open-access article distributed under the terms and conditions of the Creative Commons Attribution (CC BY) license